Detector Temperature Dependence for MESSENGER Surface Reflectance Measurements and Implications for Mercury Surface Science. Noam R. Izenberg[1], Gregory M. Holsclaw[2], Scott L. Murchie[1], Deborah L. Domingue[3], William E. McClintock[2], Sean C. Solomon[4], and the MESSENGER Team. [1]Johns Hopkins University Applied Physics Laboratory, 11100 Johns Hopkins Road, Laurel, MD 20723, USA (noam.izenberg@jhuapl.edu); [2]Laboratory for Atmospheric and Space Physics, University of Colorado, Boulder, CO 80303, USA; [3]Planetary Science Institute, Tucson, AZ 85719, USA; [4]Department of Terrestrial Magnetism, Carnegie Institution of Washington, Washington, DC 20015, USA.

Introduction: En route to its orbital mission around Mercury, the MESSENGER spacecraft flew by Mercury on January 14, 2008 (M1), October 6, 2008 (M2), and September 29, 2009 (M3). During the first two flybys, the Mercury Atmospheric and Surface Composition Spectrometer (MASCS) [1] conducted exosphere and surface observations, including spectral reflectance measurements of Mercury's surface from visible to near-infrared wavelengths at high spatial and spectral resolution.

The Visible and Infrared Spectrograph (VIRS) sensor of MASCS consists of separate visible (VIS) and infrared (IR) linear photodiode arrays covering the wavelength range 320-1450 nm. Initial resolved spectra from the flybys [2, 3] show a highly space-weathered regolith [4]; differences among surface units agree with results from color imaging with the Mercury Dual Imaging System (MDIS) [5]. Surface spectra do not exhibit a 1-μm absorption band (Fig. 1) diagnostic of Fe^{2+} in silicate minerals [6].

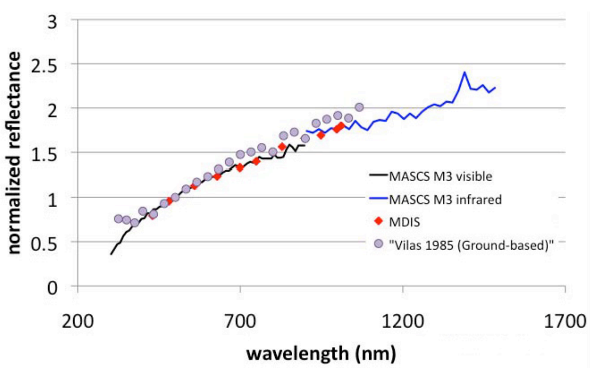

Fig. 1. MESSENGER and Earth-based observations of Mercury, at phase angles of 85°-86°. MASCS IR channels align with MDIS observations, but long-wavelength VIS channels show lower reflectance than both MDIS and MASCS IR.

Continued analysis of the VIRS calibration and the construction of photometric corrections are both necessary for inter-comparison of MASCS and MDIS data with each other and with Earth-based telescopic data [7, 8] (Fig. 1). This comparison has revealed a need to refine VIRS calibration including implementation of a correction for changes in detector response with temperature.

With laboratory calibration measurements, we created a first-generation temperature correction for the two VIRS detectors. Here we show initial implementation on resolved spectra obtained during M1 and M2, and we discuss implications for mineralogical interpretation of Mercury spectra.

Ground-based Temperature Measurements: On-ground response of the VIRS VIS detector was characterized at 11 different temperatures. Relative response of the VIS detector across its wavelength range is shown in Fig. 2. Operational temperatures for this detector during the Mercury flybys were around 10°C; temperatures in orbit are expected to vary from slightly cooler to much warmer.

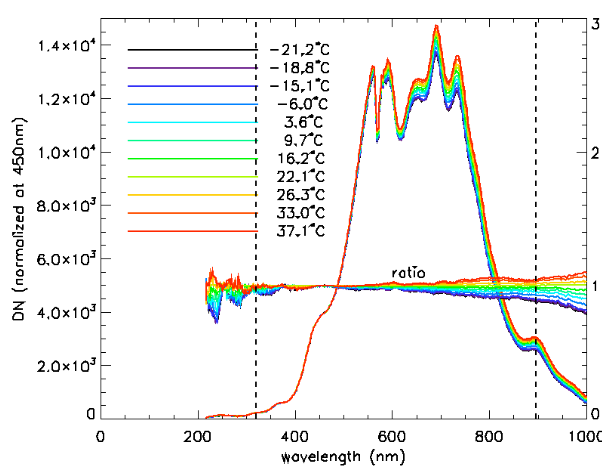

Fig. 2. Relative VIRS visible-detector response versus wavelength and temperature; left axis gives response scale and right axis the ratio to the response at 21°C, at which instrument sensitivity was derived. Vertical dashed lines show the useful wavelength interval of the detectors. The greatest temperature dependence occurs where VIS and IR data mismatch each other.

Ground-calibration measurements of the response of the VIRS infrared detector were taken at eight different temperatures. Operational temperatures for this detector during the Mercury flybys were around 14°C, and temperatures in orbit are expected to vary from slightly cooler to much warmer. The longest useful wavelength in the IR detector is 1450 nm. Warmer temperatures result in markedly increased noise in the IR.

The percentage changes with temperature relative to the temperature at which the instrument sensitivity was derived were compared. Results for the VIS detector are shown in Fig. 3. Response varies as functions of both wavelength and detector temperature; linear corrections are unsatisfactory fits in most cases, and the percentage change in response is significant over the expected operational temperature range. For the IR detector, temperature dependence is highly channel-dependent and not organized by wavelength, suggesting "flat-field" effects.

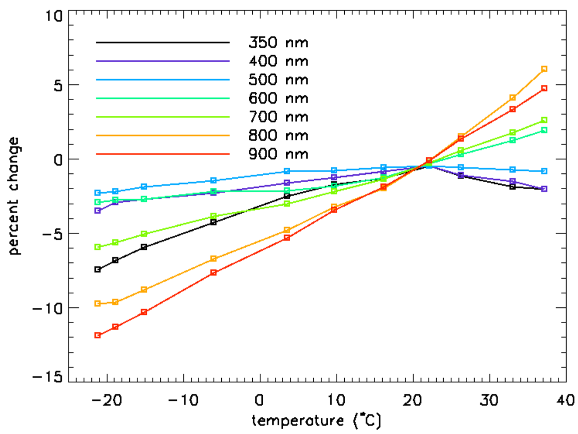

Fig. 3. Percentage change with temperature of the response of the VIRS visible channel. The IR channel has a similar set of derived response curves, with additional channel-to-channel curvature variation implying uncompensated noise or flat-field variation.

Derived Binomial Temperature Correction Matrices: We derived a set of wavelength-dependent temperature-correction factors for both VIRS detectors. Each wavelength was fit over a range of temperatures with a simple binomial of the form $F_n = c_0+c_1x+c_2x^2$.

Flyby Observations with Correction Applied: Preliminary corrections were applied to median flyby spectra from M1 and M2, as well as a combined median spectrum from both flybys. Results are shown in Fig. 4. The correction improves, but does not fully remove the discontinuity between observations near 900 nm wavelength from the VIS and IR VIRS detectors, as well as disagreement between VIRS and MDIS multispectral observations in the near infrared.

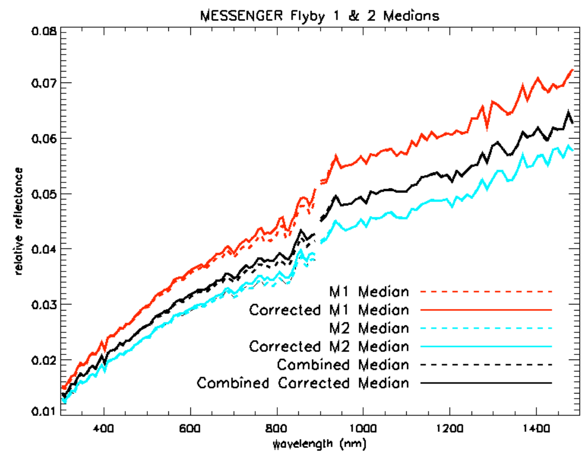

Fig. 4. Median spectra from M1 and M2 uncorrected (dashed lines) and with preliminary correction (solid lines) for detector temperature.

Implications for Mercury's Mineralogy and Future Work: We continue to improve the correction for detector temperature (e.g. refining magnitude and channel dependence) and intend to implement a version into the data calibration pipeline before MESSENGER achieves Mercury orbit. This correction, and others to follow, should improve the detectability of the 1-μm Fe^{2+} band and increase confidence regarding its presence or absence.

References: [1] W. E. McClintock and M. R. Lankton (2007) *Space Sci. Rev. 131*, 481-522; [2] W. E. McClintock et al. (2008) *Science 321*, 62-65; [3] N. R. Izenberg et al. (2009) *Lunar Planet. Sci. 40*, 1663; [4] D. T. Blewett et al. (2009) *EPSL* 285, 272-282; [5] S. E. Hawkins, III, et al. (2007) *Space Sci. Rev. 131*, 247-338; [6] R. G. Burns (1993) in *Remote Geochemical Analysis*, C. M. Pieters, P. A. J. Englert (Eds.), Cambridge Univ. Press, pp. 3-27 [7] D. L. Domingue et al. (2010) *Planet Space Sci.,* submitted; [8] F. Vilas (1985) *Icarus* 64, 133-138.